Inhibition of corrosion causing *Pseudomonas aeruginosa* using plasma activated water

Eleni Asimakopoulou[1, *], Sotirios I. Ekonomou[2], Pagona Papakonstantinou[3], Olena Doran[4], Alexandros Ch. Stratakos[5, *]

[1] School of Engineering, University of Central Lancashire, Flyde Rd, Preston, PR1 2HE, United Kingdom, (https://orcid.org/0000-0001-5644-1372), Easimakopoulou@uclan.ac.uk

[2] Centre for Research in Biosciences, Faculty of Health and Applied Sciences (HAS), University of the West of England, Coldharbour Ln, Bristol, BS16 1QY, United Kingdom (https://orcid.org/0000-0003-3010-3038), Sotirios.Oikonomou@uwe.ac.uk

[3] Engineering Research Institute, School of Engineering, Ulster University, Newtownabbey BT37 0QB, United Kingdom, (https://orcid.org/0000-0003-0019-3247), p.papakonstantinou@ulster.ac.uk

[4] Faculty of Health and Applied Sciences (HAS), University of the West of England, Coldharbour Ln, Bristol, BS16 1QY, United Kingdom (https://orcid.org/0000-0002-6391-3988), Olena.Doran@uwe.ac.uk

[5] Centre for Research in Biosciences, Faculty of Health and Applied Sciences (HAS), University of the West of England, Coldharbour Ln, Bristol, BS16 1QY, United Kingdom, (https://orcid.org/0000-0001-6117-7385), Alexandros.Stratakos@uwe.ac.uk

[*] Corresponding authors info:

Dr Eleni Asimakopoulou, email: easimakopoulou@uclan.ac.uk, telephone number: (0044) 01772 894222

Dr Alexandros Stratakos, email: alexandros.stratakos@uwe.ac.uk, telephone number: (0044) 01173284743

Running headline: Plasma activated water against microbial corrosion

Abstract

Aims: The cost of Microbiologically Influenced Corrosion (MIC) significantly affects a wide range of sectors. This study aims to assess the efficiency of a novel technology based on the use of plasma activated water (PAW) in inhibiting corrosion caused by bacteria.

Methods and Results: This study evaluated the effectiveness of PAW, produced by a plasma bubble reactor, in reducing corrosion causing *Pseudomonas aeruginosa* planktonic cells in tap water and biofilms grown onto stainless steel (SS) coupons. Planktonic cells and biofilms were treated with PAW at different discharge frequencies (500-1500 Hz) and exposure times (0-20 min). *P. aeruginosa* cells in tap water were significantly reduced after treatment, with higher exposure times and discharge frequencies achieving higher reductions. Also, PAW treatment led to a gradual reduction for young and mature biofilms, achieving >4-Log reductions after 20 min. Results were also used to develop two predictive inactivation models.

Conclusions: This work presents evidence that PAW can be used to inactivate both planktonic cells and biofilms of *P. aeruginosa*. Experimental and theoretical results also demonstrate that reduction is dependent on discharge frequency and exposure time.

Significance and Impact of the Study: This work demonstrates the potential of using PAW as means to control MIC.

KEYWORDS: plasma activated water, biofilm, intracellular ATP levels, microbial corrosion, *P. aeruginosa*.

INTRODUCTION

Metal corrosion can be significantly accelerated by the presence and activity of microorganisms, a process that is also known as biocorrosion or Microbiologically Influenced Corrosion (MIC) (Phan et al. 2021) and is responsible for 20% of metal corrosion damages (Flemming, 1996). The cost of corrosion in industrialised countries was estimated to be 3.4% of the global GDP in 2013, and if corrosion protection and design were properly applied, a 15-35% loss reduction could be achieved (Koch et al. 2016). Its direct costs affect a wide range of sectors, including agriculture, forestry and fishing, mining, manufacturing (e.g., chemical processing, nuclear, oil, gas, underground pipeline, water treatment, food production, highway maintenance, aviation, metal working, marine, shipping and fire protection), electricity supply, water supply, waste management, accommodation, and food service activities, transportation, and storage. Indirect costs are associated with environmental, regulatory, and human costs, making cost estimation even more challenging (Little et al. 2020).

Until recently, corrosion research was primarily focused on operational aspects such as the assessment of the corrosion damage and mineral deposits impact on the functionality of systems, mechanical operations of equipment and unanticipated failures (Bardal, 2004). Those are more frequently encountered in systems comprised of widely used, cost-effective, but less resistant groups of metal alloys such as carbon steels (Herrera and Videla, 2009) and stainless steels (Cheng et al. 2009). The extent of those damages and mineral deposits is influenced by both materials and the environment (Lyon, 2014).

Lately, more fundamental research was conducted aiming to investigate MIC associated phenomena and advised to approach the subject systematically by monitoring the microbial activity of single bacteria (Kermani and Harrop, 2019). Different types of aerobic and anaerobic bacteria are associated with MIC; among them, the most commonly met are the acid-producing, sulphur reducing and iron related bacteria (Su and Fuller, 2014) as well as others,

such as *Pseudomonas aeruginosa* (Li et al. 2016; Jia et al. 2017). *P. aeruginosa* MIC mechanism and associated bacteria-metal reactions have been extensively investigated, and its presence is proven to accelerate corrosion (Abdolahi et al. 2014). There are several studies that confirm its involvement in the corrosion process of different types of metals e.g., mild steel (Xu et al. 2017), stainless steel (Xu et al. 2016; Jia et al. 2017; Xu et al. 2017) and aluminium (Xu et al. 2017).

Research in MIC is spanning four main areas: diagnose, monitor, modelling and prevention. To achieve the latter, numerous treatments are customarily used, and the most common ones include sanitation, physical, chemical treatment, biological methods, use of coatings and cathodic protection (Enning and Garrelfs, 2014; Ibrahim et al. 2018; Little et al. 2020). The solution of applying coating specifically designed for each application appears to be promising, however this is not always feasible and practical. An efficient way to limit microbial growth is through physical treatment (e.g. pigging, ultraviolet irradiation, ultrasonic, chemical and biological treatments) of natural or industrial water aiming to inhibit the microorganisms responsible for causing corrosion (Little et al. 2020). Recent studies have revealed that indirect application of Cold Atmospheric Plasma (CAP) at ambient air conditions can significantly decrease the microbial load (Pasquali et al. 2016; Katsigiannis et al. 2021). Also, in recent years, a new mode of CAP, i.e., Plasma-activated Water (PAW) activities has drawn attention (Julák et al. 2012; Chen et al. 2018) as it can be applied to inhibit/kill microorganisms in surfaces and systems in an environmentally friendly, cost-effective, and practical way. Lately, the application of PAW has been investigated (Tan and Karwe, 2021) and has been proven an effective technique for inactivating inner-pipe surfaces formed biofilms, also recognised as a novel technology with significantly decreased environmental cost (Zhou et al. 2020).

Despite a large number of recent publications related to MIC, an effective and practical technological solution to tackle MIC related problems is yet to be found (Little et al. 2020). To

meet this challenge, the current experimental work aims to assess the efficiency and antimicrobial mechanism of PAW against corrosion causing *P. aeruginosa* as well as identify optimal operational conditions for PAW treatment.

MATERIALS AND METHODS

Bacterial cultivation

Experiments were conducted using PAO1, a *P. aeruginosa* strain. The *P. aeruginosa* culture was prepared in Luria-Bertani (LB) liquid medium enriched with KNO_3 (LB-NO_3). The media formulation of the agar medium LB-NO_3 included 10 g tryptone, 10 g KNO_3 5 g yeast extract, and 5 g NaCl per litre of deionised water. KNO3 was added to the LB medium to support anoxic growth of *P. aeruginosa* PAO1 (Line et al. 2014). The pH was adjusted to 7.0 by applying a solution of NaOH. To mitigate any possible O_2 entry, L-cysteine at a concentration of one hundred ppm (w/w), was added to the culture medium as O_2 scavenger. The L-cysteine solution was filter-sterilised using MF-Millipore^{TM} membrane filter of a pore size of 0.22 μm (Merck KGaA, Darmstadt, Germany) before it was added to the medium. Dissolved oxygen was removed from all liquid solutions by flushing them with filter sterilised N_2 in order to maintain anoxic growth of *P. aeruginosa*. 304 Stainless Steel (SS) sheet were used to cut the rectangular shaped coupons (1 cm x 1 cm) used in this work. Coupons were sterilised in 75% ethanol solution for 2 h, dried and exposed to UV light for 30 min prior to use. A N_2 chamber was used for anaerobic manipulations. The biofilms were grown in anaerobic vials, following the procedure described by Jia et al. (2017). One hundred ml of LB-NO_3 medium, with and without the addition of the *P. aeruginosa* culture, was added to each anaerobic vial. The experiments were conducted on three replicate coupons. The initial bacterial concentration after inoculation with *P. aeruginosa* was approximately 10^{4-5} Log CFU ml^{-1}. The vials were closed and incubated at 37^{o}C for 2, 5, or 7 days. After the incubation, the coupons were removed, and PAW treated under different conditions as described below. Before PAW

treatment, the coupons were gently rinsed with sterile phosphate-buffered saline to remove the non-adhered and loosely attached bacterial cells.

Plasma bubble reactor

A schematic representation of the plasma bubble reactor (PBR) used to generate the PAW is illustrated in Figure 1. The PBR consisted of an acrylic tube with a 140 mm length that constituted of machined caps at each end. Those caps had 4 mm stainless-steel rod positioned coaxially at the interior of the full length of the tube, acting as high voltage electrodes. A 5 mm wide strip of adhesive copper tape was positioned at the exterior of the ground electrode and was connected to the ground wire of the plasma power supply. Plasma was generated under atmospheric conditions, and the electrical discharges were provided by a high voltage power supply (PlasmaLeap Technologies, Ireland) specifically designed to supply a wide range of voltages at discharge frequencies.

The acrylic tube of the PBR, submerged into the water, was perforated with ten 2 mm holes located 8 mm from its base. Compressed air to the PBR was supplied at a flow rate of 1 l min^{-1} via a tube placed at the opposing end of the acrylic tube. The electrically discharged bubbles leaving the reactor, through the holes entered the water, and subsequently, the generated reactive species at their interior, contacted the water via their bubble surface-water interface.

PAW treatment of stainless-steel (SS) coupons and biofilm enumeration

The plasma reactor was filled with 100 ml of sterile tap water. Control SS coupons (no PAW treatment) were immersed in water and placed on the bottom of the reactor, with just the airflow on, for 15 min without igniting the plasma. For treated samples, coupons were placed in the reactor and subsequently the PBR was turned on. The reactor was allowed to run for different times (5, 10, 15, and 20 min), at 150 V (voltage applied at the high voltage transformer), 100-µs duty cycle (time during which the energy from the power supply unit is transferred to HV transformer resonance circuit) and 60 kHz resonance frequency (resonance frequency of

148 resonance circuit). Three different discharge frequencies were investigated (500, 1000, and
149 1500 Hz).
150 SS coupons with adhered biofilm cells of different maturity were treated directly in PBR for 0,
151 5, 10, 15, and 20 min. After treatment, the SS coupons were positioned in a sterile container
152 with 10 mL maximum recovery diluent (MRD) (Oxoid, UK) and 1 g glass beads caliber of 0.1
153 mm diameter. To detach the surviving biofilm cells from the SS coupons, samples were
154 vortexed for 60 s. Subsequently, 10-fold dilutions were prepared in MRD to enumerate the
155 surviving biofilm cells. An aliquot of 100-µl was used from the appropriate 10-fold serial
156 dilutions and was spread plated on Tryptone Soya Agar (TSA, Oxoid, UK). Plates were
157 incubated at 37 °C for 24 h and the biofilm cells expressed as Log CFU cm^{-2}.
158 **PAW treatment and enumeration of *P. aeruginosa***
159 *P. aeruginosa* can exist in the water before it attaches to surfaces and begin to form biofilms
160 and subsequently influence the physicochemical metal-environment interactions, thus
161 enhancing MIC (Li et al. 2016; Jia et al. 2017). To investigate if PAW can inactivate this
162 microorganisms in its planktonic form, 100-µl of the *P. aeruginosa* (prepared as described
163 above) was inoculated into 100 ml of tap water. After inoculation, the bacterial concentration
164 was approximately 10^5 Log CFU ml^{-1}. Control samples received no treatment (0 min; only
165 airflow was on for 15 min without igniting the plasma). For the rest of the PAW treatments,
166 the PBR was turned on and allowed to run for different time periods (0, 5, and 10 min) at 150
167 V, 100-µs duty cycle, 60 kHz resonance frequency and 500, 1000, and 1500 Hz discharge
168 frequencies. The planktonic cells were treated inside the reactor. Immediately after treatment,
169 an aliquot (1 ml) of the treated tap water was added to 9 ml of MRD and subsequently, further
170 suitable 10-fold dilutions were prepared. An aliquot of 100-µl was used from the appropriate
171 10-fold serial dilutions and was spread plated on Trypticase Soy Agar (TSA, Oxoid, UK).

Plates were incubated at 37 °C for 24 h, and planktonic *P. aeruginosa* cells were expressed as Log CFU ml^{-1}.

Physicochemical properties of PAW

PAW was generated at a discharge frequency of 1500 Hz for 15 minutes, and the measurements of pH, electrical conductivity (EC), H_2O_2, NO_2^-, and NO_3^- concentrations were taken immediately after treatment. Values of EC and pH were measured using an electronic conductivity meter (Jenway 4200, UK) and a pH meter (FiveEasy, Mettler Toledo, UK), respectively. H_2O_2 concentration was determined using the titanium oxysulphate ($TiOSO_4$; Sigma-Aldrich) method. According to that method, $TiOSO_4$ reacts with H_2O_2, and produces a yellow-coloured complex (pertitanic acid). Subsequently, the H_2O_2 concentration was determined spectrophotometrically (Mai-Prochnow et al. 2021b). Nitrite concentration was determined by using the Griess assay, a chemical rection that uses N-(1-naphthyl)-ethylene diamine hydrochloride under sulfanilic acidic conditions, resulting in the formation of a magenta-coloured azo dye. Nitrate (NO_3^-) concentration was determined using a nitrate assay kit (Sigma, UK) that is based on its reaction with 2, 6-dimethylphenol (DMP). To eliminate nitrite interference, all PAW samples were pre-treated using sulfamic acid (Zhao et al. 2020) prior to analysis.

Individual standard curves of known H_2O_2, $NaNO_2$ and $NaNO_3$ concentration were prepared to convert the absorbance to H_2O_2, NO_2^-, NO_3^-, concentrations.

Membrane integrity

Protein leakage was used to assess membrane integrity of *P. aeruginosa* suspension cells after PAW treatment at 500, 1000, and 1500 Hz discharge frequencies. This was achieved by measuring protein concentration in the supernatants using a Pierce BCA protein kit (ThermoScientific, U.K.) (Sadiq et al. 2017) and using untreated samples as controls.

196 **Intracellular adenosine triphosphate levels**

197 The effect of PAW treatment on the intracellular adenosine triphosphate (ATP) levels was
198 determined using the procedure described by Stratakos et al. (2018). The 24 hours old *P.*
199 *aeruginosa* cultures were centrifuged at 5000 x g for 5 min. The produced pellets were washed
200 three times using phosphate-buffered saline, and centrifugation was used to collect the cells.
201 The pellets were re-suspended in one millilitre of PAW production at PBR discharge
202 frequencies of 500, 1000, or 1500 Hz respectively for 15 min. Subsequently, all samples were
203 stored for 15 min at 37^{o}C. Cells were centrifuged at 5000 x g for 5 min and treated with a lysis
204 buffer (Roche, U.K.) for another 5 min at room temperature to extract the intracellular ATP.
205 The intracellular ATP quantity was determined with the ATP assay kit (ATP bioluminescence
206 assay kit HS II, Roche, U.K.); 100 ml of ATP luciferase reagent were added to the100 ml of
207 supernatant in solid white 96-well plates. Then to determine ATP concentrations a microplate
208 reader (FLUOstar Omega, BMG Labtech, U.K.) was used using untreated samples as controls.

209 **Statistical analysis and modelling**

210 All treatments were performed three times, and each sample was analyzed twice and averaged
211 before statistical analysis. Statistical analysis was done with Excel Microsoft® Office 365 (ver.
212 16.48). Tukey post hoc tests were used to compare sample data using the IBM® SPSS®
213 statistics 26 software for macOS (SPSS Inc., US). A 5.0 % level of significance, *P*, was used,
214 and thus results were considered statistically significant when *P* was less than 0.05 ($P < 0.05$).
215 The fitting procedure for modelling of inactivation kinetics was performed using GInaFiT
216 software (Geeraerd et al. 2005).

217 **RESULTS**

218 **The efficacy of PAW treatment against planktonic cells of *P. aeruginosa***

219 The effect of PAW treatment on planktonic *P. aeruginosa* cells after 5, 10, and 15 min exposure
220 to different PBR discharge frequencies (500, 1000, and 1500 Hz) is presented in Figure 2. The

initial population of *P. aeruginosa* control cells without plasma treatment in tap water was 4.99 Log CFU ml^{-1}.

The population of *P. aeruginosa* in tap water was significantly reduced after 5 min of PAW treatment and reached 0.44, 1.77, and 2.51 Log CFU ml^{-1} at 500, 1000 and 1500 Hz, PBR discharge frequencies respectively (Fig 2, $P < 0.05$). *P. aeruginosa* cells, treated with PAW for 10 min resulted in a significant reduction of the cell numbers by 1.26 and 2.88 Log CFU ml^{-1} at 500 and 1000 Hz, respectively (Fig 2, $P < 0.05$). However, PAW treatment at 1500 Hz resulted in a reduction below the detection limit (>3.99 Log CFU ml^{-1}) (Fig 2). After 15 min of PAW treatment at 1000 and 1500 Hz, the bacterial numbers of *P. aeruginosa* were reduced below the detection limit, while PAW treatment at 500 Hz resulted in a significant reduction, of 1.69 Log CFU ml^{-1} (Fig 2, $P < 0.05$).

The reduction of *P. aeruginosa* planktonic cells under the investigated discharge frequencies of PAW treatment depended on the exposure time. As shown in Fig 2, all the PAW treatments resulted in a significant decrease in the number of the planktonic cells after 5- and 10-min exposure (Fig 2, $P < 0.05$). In the case of *P. aeruginosa* cells treated at 500 Hz, significant bacterial reduction was observed for all the exposure times investigated. There were no significant differences between the effect of plasma treatments at 1000 and 1500 Hz (neither at 10 nor 15 min) when bacterial numbers were reduced close to or below the detection limit (Fig 2, $P > 0.05$).

The efficacy of PAW treatment against biofilms of *P. aeruginosa*

P. aeruginosa can form biofilms on the surface of stainless-steel pipes, accelerating MIC (Jia et al. 2017). This study investigated whether PAW treatment can be applied to reduce the more resistant *P. aeruginosa* biofilms. To assess the efficacy of PAW treatment, further experiments were carried out using the most effective PBR discharge frequency of 1500 Hz against the biofilms of *P. aeruginosa* grown on stainless-steel coupons for 24, 48, and 72 h. Reduction

levels of *P. aeruginosa* biofilms are presented in Figure 3. Plasma discharge in bubbles for 5 min reduced the 24, 48, and 72 h attached biofilm cells of *P. aeruginosa* by 2.77, 2.20, and 1.42 Log CFU $cm^{2\ -1}$, respectively (Fig 3, $P < 0.05$). The same trend was observed after 10 min of PAW treatment with increased efficacy, where bacterial numbers for biofilms grown for 24, 48, and 72 h were reduced significantly by 3.77, 3.12, and 2.55 Log CFU $cm^{2\ -1}$, respectively (Fig 3, $P < 0.05$). After 15 min of exposure, the 24 h old biofilms were reduced by >4.00 Log CFU cm^{-2}, below the detection limit of 2.00 Log CFU cm^{-2} (Fig 3). However, *P. aeruginosa* 48 and 72 h mature biofilms decreased below the detection limit (2.00 Log CFU $cm^{2\ -1}$) after 20 min of exposure at PAW treatment, corresponding to >4.15 and >4.24 log reduction of CFUcm^{-2} (Fig 3).

There was a significant reduction in bacteria population for the 24 h biofilms, exposed for 5 and 10 min (Fig 3, $P < 0.05$). In addition, *P. aeruginosa* 48 and 72 h mature biofilms showed significant differences in reductions achieved at all the PAW exposure times (Fig 3, $P < 0.05$).

Physicochemical properties of PAW treatment

The PBR that was used to generate PAW at 1500 Hz discharge frequency and 15 min of exposure time produced different reactive species. The physicochemical properties of PAW treatment are shown in Table 1. The initial pH value of the tap water was 7.56±0.024, which decreased to 5.94±0.038 after 15 min exposure ($P < 0.05$). Also, the EC value of the water significantly increased ($P < 0.05$), which suggests the formation of reactive molecular species under these conditions. The specific reactive species, produced as the result of complex chemical reactions between the plasma and liquid (tap water), that were detected and quantified were H_2O_2 (0.028±0.002 mg ml^{-1}), NO^{2-} (0.037± 0.001 mg ml^{-1}), and NO^{3-} (0.039± 0.001 mg ml^{-1}).

Effect of PAW treatment on *P. aeruginosa* protein release

Data in Figure 4 show the amount of protein released from *P. aeruginosa* planktonic cells treated with PAW at 500, 1000, and 1500 Hz of PBR discharge frequency. Protein leakage from PAW-treated *P. aeruginosa* cells at 1000 and 1500 Hz significantly increased compared to that from untreated cells (control) and from the cells treated at 500 Hz (Fig 4, $P < 0.05$). The highest release of proteins for the PAW-treated *P. aeruginosa* planktonic cells was observed at 1000 and 1500 Hz, respectively. The data suggest that there was a gradual increase in protein release in the cell suspension with increase in discharge frequency.

Effect of PAW treatment on *P. aeruginosa* intracellular ATP levels

Results on the effect of PAW treatment on *P. aeruginosa* Intracellular ATP levels at different discharge frequencies are presented in Figure 5. The ATP calibration curve showed a positive linear relationship between relative luminescence units and ATP level, which can be described by the following equation: $y = 475926x + 22826$; $R^2 = 0.986$. The level of intracellular ATP of *P. aeruginosa* decreased significantly as the discharge level of PAW treatment increased from 500 to 1000 and 1500 Hz (Fig 5, $P < 0.05$). The initial ATP concentration of the untreated (Control) *P. aeruginosa* cells was 0.340 mM, while after PAW treatment at 500, 1000, and 1500 Hz, it was reduced to 0.164, 0.073, and 0.042 mM, respectively ($P < 0.05$).

Modelling of inactivation kinetics

The responses of the different parameters in the microbial population of *P. aeruginosa* to different exposure times were fitted using a log-linear regression model (Bigelow and Etsy, 1920). Analysis of the experimental dataset of the microbial population of *P. aeruginosa* was performed using a weighted least square linear fit model. The Coefficient of Determination (COD), also known as R^2, was used as a statistical measure to assess the quality of each linear regression fit. The linear regression model, Equation (1), was used to estimate the kinetic inactivation parameter, D_T, for the different PBR discharge frequencies for the planktonic *P.*

aeruginosa cells and the young, 24 h old, and mature, 48 and 72 h old, biofilms. In the Equation (1), N represents the microbial population at time t, and N_o is the experimentally determined initial microbial population. Microbial population measurements below the level of detection (D) were handled using a substitution method (Ogden, 2010). According to the substitution method every result below D, also known as censored data, is substituted with an estimate, for what it might be. Traditional options for handling censored data include discarding non-detect data and using simple substitution methods (treating non-detects as zero, half the detection limit, at the detection limit, or the detection limit/$\sqrt{2}$) (Levine et al. 2009; EPA, 2006). Instead of eliminating censored data from the data set, setting them as zero or D values, that has been proved to yield erroneous results (Silvestri et al. 2017), in the current study values bellow D, were substituted with $D/2$ (Levine, 2006; Ogden, 2010).

Tables 2 and 3 present the model parameters and their measures of statistical dispersion namely the standard error (SE), mean sum of R^2, root mean sum of R^2, R^2 and adjusted R^2 for biofilms of different maturity and PBR discharge frequencies. Figure 6 shows the relevant fitted inactivation curves for biofilms of *P. aeruginosa* grown for 24, 48, and 72 h and treated with PAW at a discharge frequency of 1500 Hz. The developed model can be reliably used to describe the inactivation curves. Good statistical fit was observed for biofilms of different maturity with estimated adjusted R^2 values ranging from 0.9005 to 0.9445. The calculated values for the inactivation parameter D_T for each biofilm ranged from 3.11 for the 24 h old biofilms to 4.34 for the 48 h old biofilms. The relevant model parameters and associated errors for *P. aeruginosa* planktonic cells after PAW treatment at different PBR discharge frequencies are presented in Table 3. Figure 7 shows the inactivation curves for the different exposure times. The inactivation parameter D_T tends to decrease with the increase of PBR discharge frequencies, with the values ranging from 8.53 at 500 Hz to 2.24 at 1500 Hz. The accuracy of

318 the developed model is supported by the statistical parameters and evaluation of the fitting
319 curves (Fig 7).

320 $$logN = logN_o - \frac{t}{D_T} \quad (1)$$

321 **DISCUSSION**

322 MIC is a destructive phenomenon that affects stainless-steel surfaces, which are widely used
323 by a range of industries, including the companies producing material for various equipment or
324 building purposes. This study proposes an innovative approach to tackle the issue of MIC.
325 The approach is based on the application of PAW against *P. aeruginosa*, which is known to
326 cause corrosion on stainless-steel surfaces (Gabriel et al. 2016). Although, corrosion inhibition
327 itself from *P. aeruginosa* was not assessed, this work presents the first evidence that PAW is
328 effective in inactivating both planktonic cells and biofilms of *P. aeruginosa* grown under
329 anaerobic conditions. Furthermore, the results of this study were rationalized by means of two
330 predictive inactivation models.

331 During the last decade, cold plasma treatment has been attracting attention as a green
332 technology for the inactivation of spoilage and pathogenic bacteria on different matrices
333 (Ehlbeck et al. 2010; Pasquali et al. 2016; Jayathunge et al. 2019; Ekonomou and Boziaris,
334 2021), as well as a method for decontamination of industrial surfaces and medical equipment
335 (Ben Belgacem et al. 2017; Alshraiedeh et al. 2020; Gonzalez-Gonzalez et al. 2021). Recently,
336 the development of PAW offered a new opportunity as a promising decontamination method
337 for the preservation of food (Ma et al. 2015; Liao et al. 2018; Thirumdas et al. 2018) and wound
338 healing in the medical industry (Chen et al. 2017; Kaushik et a., 2017), and as an alternative
339 disinfectant for the inactivation of bacteria in water (Pan et al. 2017; Zhou et al. 2018). In this
340 work, PAW showed a high antimicrobial effect against planktonic cells of *P. aeruginosa*. The
341 efficacy of the treatment increased by extending the cells' exposure time to PAW and applying
342 higher PBR discharge frequencies. The highest reduction of the planktonic cells was observed

343 at 1500 Hz when the number of cells was below the detection level of 1.00 Log CFU ml^{-1}. Our
344 results agree with the study by Xiang et al. (2018), who reported that PAW produced by a
345 pressure plasma jet system (input power set at 750 W) effectively inactivated *P. deceptionensis*
346 CM2 planktonic cells in a time-dependent manner. Similarly, Tan and Karwe (2021) observed
347 the reduction of *Enterobacter aerogenes* planktonic cells floating in a pipe system after PAW
348 by approximately 3.50 Log CFU ml^{-1}. Inhibition of corrosive bacteria, e.g. *P. aeruginosa,* in
349 the water phase is a critical step in avoiding further colonization of industrial or medical
350 surfaces and interaction with other bacteria, fungi and viruses that can cause severe infections
351 in humans (Smith et al. 2015; Hendricks et al. 2016). It is important to highlight that the ability
352 of *P. aeruginosa* to grow and co-exist with other microorganisms in communal biofilms has
353 been associated with increased resistance against antimicrobials and disinfection strategies
354 (Pinto et al. 2020; del Mar Cendra and Torrents, 2021). Usually, the origin of bacterial
355 inactivation is linked to the formation of specific molecules during PAW generation (e.g.,
356 H_2O_2, nitrate and nitrite). However, it has also been shown that the transient electric fields
357 linked to the generation of cold plasma/plasma activated liquids can induce membrane
358 permeabilization, which can also contribute to cell damage and death (Naidis, 2010; Zhang, et
359 al. 2014; Robert et al. 2015; Chung et al. 2020; Vijayarangan et al. 2020; Dozias et al. 2021).
360 The inactivation depends on several factors such as bacterial species (gram-positive or negative
361 strains), physiological state of the microorganism (exponential or stationary growth), the
362 growth medium and the mode of growth (planktonic or biofilm) (Smet et al. 2019; Mai-
363 Prochnow et al. 2021a).
364 To investigate the mechanism of the antimicrobial effect of PAW on *P. aeruginosa,* the
365 intracellular ATP levels were monitored. ATP is required for many essential cellular functions
366 such as growth, replication, and survival (Shi et al. 2016). PAW treatment significantly reduced
367 the intercellular ATP levels of planktonic *P. aeruginosa* cells, and this ATP reduction increased

368 with PBR discharge frequencies. These results are consistent with Qian et al. (2021)
369 observations, who showed that cold plasma treatment decreased the ATP levels of *L.*
370 *monocytogenes* and *S. Enteritidis* cells. The reduction of intracellular ATP in *P. aeruginosa*
371 observed in our study could be attributed to an increase in the cell membrane permeability and
372 the resulting ATP leakage (Bajpai et al. 2013). Also, our study demonstrated that PAW
373 treatment resulted in protein leakage from the cells, suggesting a gradual increase in the
374 bacterial cell membrane permeability with an increase in PBR discharge frequency. This might
375 be due to the damage of the membrane by the increasing levels of the reactive species produced
376 in PAW.
377 Application of PAW as a treatment against the biofilms of gram-negative and gram-positive
378 bacteria is an emerging field of study (Chen et al. 2017; Kaushik et al. 2018). Our study also
379 investigated the effect of PAW on the more resistant biofilms of *P. aeruginosa*. The most
380 effective PBR discharge frequency of (1500 Hz) was used against different maturity biofilms
381 levels grown on SS surfaces. Numerous studies have previously described the mechanism of
382 biofilm formation by *P. aeruginosa* (Morales et al. 1993; Klausen et al. 2003; Yuan et al. 2007;
383 Harmsen et al. 2010) and their strong ability to further oxidize the substrate, thus leading to
384 severe pitting corrosion (Yuan et al. 2008; Hamzah et al. 2013). It is known that *P. aeruginosa*
385 biofilms can lead to microbial corrosion of different steel types such as SS 316 and 304
386 (Hamzah et al. 2013; Gabriel et al. 2016), C1018 (Jia et al. 2017), and other metallic surfaces
387 (Beech and Sunner, 2004; Wang et al. 2004; González et al. 2019). This study showed that
388 PAW treatment significantly reduces the level of bacterial cells and that this reduction
389 depended on the maturity of the biofilms. Patange et al. (2021) demonstrated inactivation of
390 early and mature *Escherichia coli* and *Listeria innocua* biofilm cells by atmospheric air plasma
391 (AAP). They showed that a 5 min AAP treatment reduced the cell count by approximately 3.5
392 to 4.5 Log CFU ml^{-1}. Gabriel et al. (2016) reported a 5-Log reduction of *P. aeruginosa* biofilm

cells on SS type 304 and 316 with different surface finishes after treatment with atmospheric plasma for 90 s. Castro et al. (2021) investigated the removal of *P. fluorescens* and *P. aeruginosa* biofilm cells; they used peracetic acid, sodium hypochlorite and Chlorhexidine digluconate at concentrations recommended by the manufacturers and observed a much lower than 5-Log cycles reduction. As a general observation, chlorine disinfection requires a relatively longer time to reach a similar Log reduction compared to PAW treatment. This can be attributed to chlorine's lower ability to disrupt the biofilm cells' exopolysaccharide (EPS) matrix (Myszka and Czaczyk, 2011). Therefore, these findings demonstrate a strong potential of PAW treatment against microorganisms that can cause microbial corrosion in the absence of carcinogenic and mutagenic chlorine compounds (Meireles et al. 2016; Thorman et al. 2018).

PAW is considered a promising technology, showing apparent suitability to substitute more traditional treatments used in a wide range of sectors, e.g. chlorine-based (Xiang et al. 2018; Pantage et al. 2021). However, as PAW is yet a novel technology, a detailed investigation of its mechanism of action and potential interactions with EPS matrix and other biofilm compounds is yet to be performed. It is well known that biofilm maturity significantly affects plasma penetration because thicker biofilms with more biomass provide a better protection against reactive species (Chen et al. 2017; Hathaway et al. 2019; Patange et al. 2021). The same effect was observed in the current study, when the 72 h mature biofilms were found to be most resistant against PAW treatment. The presence of a complex mix of many reactive species in PAW has been described as a significant antimicrobial factor affecting matrix degradation (Tian et al. 2015; Cherny et al. 2020; Mai-Prochnow et al. 2021a). When the matrix is disrupted, it is observed that biofilm cells can detach as either individual cells or larger cell clusters, thus leaving small gaps in the biofilm structure (Mai-Prochnow et al. 2004). This proposed mechanism of PAW interaction with biofilms relies on the reactive species to disrupt

418 the EPS matrix and release the sessile cells that can change their physiological state back to a
419 more susceptible planktonic state. Furthermore, Li et al. (2019) have shown that biofilm
420 treatment with PAW can downregulate the virulence genes linked to quorum sensing,
421 presenting an opportunity for the disruption and removal of biofilm cells.
422 The nature and amount of reactive species produced in PAW vary depending on the methods
423 used to generate them, which affects the PAW efficacy in various applications (Chen et al.
424 2018; Thirumdas et al. 2018; Zhou et al. 2020). PAW efficacy will also be influenced by
425 storage time and conditions (Zhao et al. 2020), which should be taken into since there could be
426 a delay between PAW generation and application. Plasma represents a highly reactive
427 environment, and in the case of PAW, the main reactive species present are hydroxyl radicals
428 (OH•), hydrogen peroxide (H_2O_2), ozone (O_3), superoxide (O_2^-), nitric oxide (NO•) and
429 peroxynitrite (ONOOH) all with a crucial role in bacterial inactivation (Han et al. 2016; Mai-
430 Prochnow et al. 2021a). However, some short-lived reactive species present, such as hydroxyl
431 radicals (OH•), singlet oxygen ($^1O_2$), and superoxide (O_2^-) also have shown to contribute to
432 microbial inactivation although to a lesser extent (Surowsky et al. 2016; Liao et al. 2018).
433 Hydrogen peroxide (H_2O_2) monitored in the current study is one of the most common long-
434 lived reactive species found in PAW, which, together with nitrite (NO_2^-) and nitrate (NO_3^-),
435 play a significant role in microbial inactivation and biofilm removal (Park et al. 2017). In the
436 current study, nitrate followed by nitrite anions showed the highest concentrations among the
437 reactive species identified, illustrating the potential high efficacy of the PAW treatment against
438 *P. aeruginosa* planktonic cells and biofilms at 1500 Hz for 15 min. This is consistent with data
439 from other studies reporting that long-lived NO_2^-, NO_3^-, and H_2O_2 reactive species are efficient
440 against a wide range of bacteria, that can contaminate different types of surfaces (Naïtali et al.
441 2010; Shen et al. 2016; Xiang et al. 2018; Zhao et al. 2020). Mai-Prochnow et al. (2021b)
442 recently proved that a higher PBR discharge frequency leads to a higher production of reactive

443 species. The present study demonstrated that the higher level of reactive species generated with
444 the highest PAW treatment frequency leads to increased bacterial inactivation.
445 The higher EC observed in the current study provided further evidence for the accumulation of
446 the reactive species in PAW, leading to high inactivation of both planktonic cells and biofilms
447 of *P. aeruginosa*. The plasma treatment resulted in a significant drop in the pH of PAW,
448 however, the final pH was not low enough to be considered as a contributing factor to
449 antimicrobial activity. The extent of the pH drop observed, can be explained by the fact that
450 tap water was used to produce PAW and that its initial pH was approximately 7.56. Also, it
451 could possibly be attributed to H^+ reacting with the different components in PAW and thus
452 result in a less pronounced pH drop. Bacteria inactivation mechanism in liquids is a result of
453 complex interactions at the plasma/gas–liquid-interface. The same applied for the subsequent
454 reactions in the liquid volume, and these interactions have not yet been fully described
455 (Oehmigen et al. 2011; Xiang et al. 2018).
456 Application of modelling can be beneficial for developing MIC mitigating strategies. As far as
457 inactivation of microorganisms in water systems is concerned, dynamic modelling has been
458 recently used to evaluate the thermal inactivation of *L. pneumophila* in water and proved an
459 efficient preventive approach for plumbing systems (Papagianeli et al. 2021). In the current
460 study, the log linear model developed confirmed our experimental results showing that PAW
461 treatment at 1500 Hz is the most effective with a Dt value of 2.24 comparing with 8.53 at 500
462 Hz against the planktonic cells of *P. aeruginosa*. Apparently, such trend may be associated
463 with the reactive species produced at PAW at different PBR discharge frequencies. The mature
464 (48 h and 72 h) biofilms were the most resistant, while according to the weighted least square
465 linear fit model (R^2), the models had a good fit to the experimental data. Several factors affect
466 biofilm removal, and little is known about the relationship between the level of maturity and
467 the treatment exposure. Our results can provide valuable data on the inhibition of the planktonic

cells of *P. aeruginosa* that can colonise the metallic surfaces creating corrosive biofilms or even removing the most resistant biofilms with PAW treatment.

This work has highlighted the efficiency of the PAW treatment against planktonic cells and biofilms of *P. aeruginosa* grown on stainless-steel coupons. Reduction of intracellular ATP levels and increase in protein release in of *P. aeruginosa cells* was attributed to an increased membrane permeability due to the effect of reactive species in PAW. The 72 h mature biofilms were found to be most resistant against PAW treatment compared to younger biofilms. The observed reduction in the number of bacterial cells indicate the potential of the PAW as a means for reduction of *P. aeruginosa* planktonic cells as well as biofilms grown on stainless-steel contact surfaces. Results of this research demonstrate that this novel methodology can be effectively used as an environmentally friendly method to inhibit MIC. A potential way to apply this technology in a practical way to inhibit MIC would be by flushing existing pipe systems with PAW or by generating PAW inside the pipe system. However, if the former application method is used then the stability of the PAW between production and application will have to be determined. Future work will focus on assessing the efficacy of PAW treatment against other microorganisms causing corrosion in specific applications such as fire engineering sprinkler maintenance, and pipe system maintenance in the food and medical industries that contribute to MIC.

ACKNOWLEDGEMENTS

This work was supported by the University of West of England -Bristol internal funding awarded to Alexandros Ch. Stratakos.

CONFLICT OF INTEREST

The authors declare no conflict of interest.

AUTHOR CONTRIBUTIONS

Eleni Asimakopoulou: Methodology, Software, Formal analysis, Data curation, Investigation, Writing – original draft, Writing – review & editing. **Sotirios I. Ekonomou:** Methodology, Formal analysis, Investigation, Data curation, Writing – original draft, Writing – review & editing. **Pagona Papakonstantinou**: Investigation, Writing – review & editing. **Olena Doran:** Methodology, Investigation, Writing – review & editing, Supervision. **Alexandros Ch. Stratakos:** Conceptualization, Methodology, Investigation, Writing – review & editing, Supervision, Funding acquisition.

DATA AVAILABILITY STATEMENT

The data that support the findings of this study are available from the corresponding author upon reasonable request.

REFERENCES

Abdolahi, A., Hamzah, E., Ibrahim, Z. and Hashim, S. (2014). Microbially influenced corrosion of steels by Pseudomonas aeruginosa. *Corrosion Reviews*, *32*(3-4), pp.129-141.

Alshraiedeh, N. A. H., Kelly, S. A., Thompson, T. P., Flynn, P. B., Tunney, M. M., Gilmore, B. F. (2020). Extracellular polymeric substance-mediated tolerance of Pseudomonas aeruginosa biofilms to atmospheric pressure non-thermal plasma treatment. *Plasma Processes and Polymers*, *17*(12), 2000108.

Bajpai, V. K., Sharma, A., Baek, K. H. (2013). Antibacterial mode of action of Cudrania tricuspidata fruit essential oil, affecting membrane permeability and surface characteristics of food-borne pathogens. *Food control*, 32(2), 582-590.

Bardal, E., 2007. *Corrosion and protection*. Springer Science & Business Media.

Beech, I. B., Sunner, J. (2004). Biocorrosion: towards understanding interactions between biofilms and metals. *Current opinion in Biotechnology*, *15*(3), 181-186.

Ben Belgacem, Z., Carré, G., Charpentier, E., Le-Bras, F., Maho, T., Robert, E., Pouvesle, J.M., Polidor, F., Gangloff, S.C., Boudifa, M. and Gelle, M.P. (2017). Innovative non-thermal plasma disinfection process inside sealed bags: Assessment of bactericidal and sporicidal effectiveness in regard to current sterilization norms. *PLoS One*, *12*(6), e0180183.

Bigelow, W. D., Esty, J. R. (1920). The thermal death point in relation to time of thermophilic microorganisms. *The Journal of Infectious Diseases*, 602-617.

Bourke, P., Ziuzina, D., Han, L., Cullen, P. J., & Gilmore, B. F. (2017). Microbiological interactions with cold plasma. *Journal of applied microbiology*, *123*(2), 308-324.

Castro, M. S. R., da Silva Fernandes, M., Kabuki, D. Y., Kuaye, A. Y. (2021). Modelling Pseudomonas fluorescens and Pseudomonas aeruginosa biofilm formation on stainless steel surfaces and controlling through sanitisers. *International Dairy Journal*, *114*, 104945.

Chen, T.P., Liang, J. and Su, T.L. (2018). Plasma-activated water: antibacterial activity and artifacts?. Environmental Science and Pollution Research, 25(27), pp.26699-26706.

Chen, T. P., Su, T. L., Liang, J. (2017). Plasma-activated solutions for bacteria and biofilm inactivation. *Current Bioactive Compounds*, *13*(1), 59-65.

Cheng, S., Tian, J., Chen, S., Lei, Y., Chang, X., Liu, T. and Yin, Y. (2009). Microbially influenced corrosion of stainless steel by marine bacterium Vibrio natriegens:(I) Corrosion behavior. *Materials Science and Engineering: C*, *29*(3), pp.751-755.

Cherny, K. E., Sauer, K. (2020). Untethering and degradation of the polysaccharide matrix are essential steps in the dispersion response of Pseudomonas aeruginosa biofilms. *Journal of bacteriology*, 202(3).

Chung, T.H., Stancampiano, A., Sklias, K., Gazeli, K., André, F.M., Dozias, S., Douat, C., Pouvesle, J.M., Santos Sousa, J., Robert, E. and Mir, L.M. (2020). Cell electropermeabilisation enhancement by non-thermal-plasma-treated pbs. *Cancers*, *12*(1), 219

del Mar Cendra, M., Torrents, E. (2021). Pseudomonas aeruginosa biofilms and their partners in crime. *Biotechnology Advances*, 107734.

Dozias, S., Pouvesle, J. M. and Robert, E., (2021). Comment on 'Mapping the electric field vector of guided ionization waves at atmospheric pressure', (2020) Plasma Res. Express 2 025014. Plasma Research Express, 3(3), p.038001.

Ekonomou, S. I., Boziaris, I. S. (2021). Non-Thermal Methods for Ensuring the Microbiological Quality and Safety of Seafood. *Applied Sciences, 11*(2), 833.

Ehlbeck, J., Schnabel, U., Polak, M., Winter, J., Von Woedtke, T., Brandenburg, R., Von dem Hagen, T. and Weltmann, K.D. (2010). Low temperature atmospheric pressure plasma sources for microbial decontamination. *Journal of Physics D: Applied Physics*, *44*(1), 013002.

EPA (2006) Data Quality Assessment: Statistical Methods for Practitioners, U.S. Environmental Protection Agency, EPA QA/G-9S.

Enning, D. and Garrelfs, J. (2014). Corrosion of iron by sulfate-reducing bacteria: new views of an old problem. *Applied and environmental microbiology*, *80*(4), pp.1226-1236.

Flemming H. C. (1996). Economical and technical overview. In: Heitz E, Flemming H-C, Sand W, Microbially influenced corrosion of materials, New York: *Springer*, 5–14.

Gabriel, A. A., Ugay, M. C. C. F., Siringan, M. A. T., Rosario, L. M. D., Tumlos, R. B., Ramos, H. J. (2016). Atmospheric pressure plasma jet inactivation of *Pseudomonas aeruginosa* biofilms on stainless steel surfaces. *Innovative Food Science and Emerging Technologies, 36,* 311-319.

Geeraerd, A.H., Valdramidis, V. P., Van Impe, J. F. (2005). GInaFiT, a freeware tool to assess non log-linear microbial survivor curves. *International Journal of Food Microbiology, 102*, 95-105.

564 Gonzalez-Gonzalez, C. R., Hindle, B. J., Saad, S., Stratakos, A. C. (2021). Inactivation of
565 Listeria monocytogenes and Salmonella on Stainless Steel by a Piezoelectric Cold
566 Atmospheric Plasma Generator. *Applied Sciences*, *11*(8), 3567.
567 González, E.A., Leiva, N., Vejar, N., Sancy, M., Gulppi, M., Azócar, M.I., Gomez, G.,
568 Tamayo, L., Zhou, X., Thompson, G.E. and Páez, M.A. (2019). Sol–gel coatings doped with
569 encapsulated silver nanoparticles: inhibition of biocorrosion on 2024-T3 aluminum alloy
570 promoted by Pseudomonas aeruginosa. *Journal of Materials Research and Technology*, *8*(2),
571 pp.1809-1818.

572 Hamzah, E., Hussain, M. Z., Ibrahim, Z., Abdolahi, A. (2013). Influence of Pseudomonas
573 aeruginosa bacteria on corrosion resistance of 304 stainless steel. *Corrosion engineering,*
574 *science and technology*, *48*(2), 116-120.
575 Han, L., Boehm, D., Patil, S., Cullen, P. J., Bourke, P. (2016). Assessing stress responses to
576 atmospheric cold plasma exposure using Escherichia coli knock-out mutants. *Journal of*
577 *applied microbiology*, 121(2), 352-363.
578 Harmsen, M., Yang, L., Pamp, S. J., Tolker-Nielsen, T. (2010). An update on Pseudomonas
579 aeruginosa biofilm formation, tolerance, and dispersal. *FEMS Immunology & Medical*
580 *Microbiology*, *59*(3), 253-268.
581 Hathaway, H.J., Patenall, B.L., Thet, N.T., Sedgwick, A.C., Williams, G.T., Jenkins, A.T.A.,
582 Allinson, S.L. and Short, R.D. (2019). Delivery and quantification of hydrogen peroxide
583 generated via cold atmospheric pressure plasma through biological material. *Journal of Physics*
584 *D: Applied Physics*, *52*(50), p.505203.

585 Hendricks, M.R., Lashua, L.P., Fischer, D.K., Flitter, B.A., Eichinger, K.M., Durbin, J.E.,
586 Sarkar, S.N., Coyne, C.B., Empey, K.M. and Bomberger, J.M. (2016). Respiratory syncytial
587 virus infection enhances Pseudomonas aeruginosa biofilm growth through dysregulation of

588 nutritional immunity. *Proceedings of the National Academy of Sciences*, *113*(6), pp.1642-
589 1647.

590 Herrera L. K., Videla H. A. (2009). Role of iron-reducing bacteria in corrosion and protection
591 of carbon steel. *International Biodeterioration and Biodegradation*, 63, 891 – 895
592 (https://doi.org/10.1016/j.ibiod.2009.06.003).

593 Ibrahim A., Hawboldt K., Bottaro C., Khan F. (2018). Review and analysis of
594 microbiologically influenced corrosion: the chemical environment in oil and gas facilities,
595 *Corrosion Engineering, Science and Technology*, 53(8), 549-563
596 (https://doi.org/10.1080/1478422X.2018.1511326).

597 Jayathunge, K. G. L. R., Stratakos, A. C., Delgado-Pando, G., Koidis, A. (2019). Thermal and
598 non-thermal processing technologies on intrinsic and extrinsic quality factors of tomato
599 products: A review. *Journal of Food Processing and Preservation*, 43(3), e13901.

600 Jia, R., Yang, D., Xu, J., Xu, D., & Gu, T. (2017). Microbiologically influenced corrosion of
601 C1018 carbon steel by nitrate reducing *Pseudomonas aeruginosa* biofilm under organic carbon
602 starvation. *Corrosion Science*, *127*, 1-9.

603 Jia, R., Yang, D., Xu, D., & Gu, T. (2017). Anaerobic corrosion of 304 stainless steel caused
604 by the Pseudomonas aeruginosa biofilm. *Frontiers in microbiology*, *8*, 2335.

605 Julák, J., Scholtz, V., Kotúčová, S., & Janoušková, O. (2012). The persistent microbicidal
606 effect in water exposed to the corona discharge. *Physica Medica*, *28*(3), 230-239.

607 Katsigiannis, A. S., Bayliss, D. L., & Walsh, J. L. (2021). Cold plasma decontamination of
608 stainless steel food processing surfaces assessed using an industrial disinfection protocol. *Food*
609 *Control*, *121*, 107543.

610 Kaushik, N. K., Ghimire, B., Li, Y., Adhikari, M., Veerana, M., Kaushik, N., ... & Choi, E. H.
611 (2018). Biological and medical applications of plasma-activated media, water and solutions.
612 *Biological chemistry*, *400*(1), 39-62.

613 Kermani B., Harrop D. (2019). Corrosion and materials in hydrocarbon production: a
614 compendium of operational and engineering aspects, *John Wiley, and Sons*.
615 Klausen, M., Heydorn, A., Ragas, P., Lambertsen, L., Aaes-Jørgensen, A., Molin, S., Tolker-
616 Nielsen, T. (2003). Biofilm formation by Pseudomonas aeruginosa wild type, flagella and type
617 IV pili mutants. *Molecular microbiology*, *48*(6), 1511-1524.
618 Koch G., Varmey J., Thompson N., Moghissi O., Gould M., Payer J. (2016). International
619 measures of prevention, application, and economics of corrosion technologies study, Gretchen
620 Jacobson, *NACE International*, Houston, Texas, USA.
621 Levine, A. D., Harwood, V. J., Fox, G. A. (2009). Collecting, Exploring, and Interpreting
622 Microbiological Data Associated with Reclaimed Water Systems. *Water Environment*
623 *Research Foundation*: Alexandria, VA, USA.
624 Li, Y., Pan, J., Wu, D., Tian, Y., Zhang, J., Fang, J. (2019). Regulation of Enterococcus faecalis
625 biofilm formation and quorum sensing related virulence factors with ultra-low dose reactive
626 species produced by plasma activated water. *Plasma Chemistry and Plasma Processing*, 39(1),
627 35-49.
628 Li H., Zhou E., Zhang D., Xu D., Xia J., Yang C., Feng H., Jiang Z., Li X., Gu T., Yang K.
629 (2016). Microbiologically Influenced Corrosion of 2707 Hyper-Duplex Stainless Steel by
630 Marine Pseudomonas aeruginosa Biofilm. *Scientific Reports*, 6, 20190.
631 Liao, X., Su, Y., Liu, D., Chen, S., Hu, Y., Ye, X., Wang, J. and Ding, T. (2018). Application
632 of atmospheric cold plasma-activated water (PAW) ice for preservation of shrimps
633 (*Metapenaeus ensis). Food Control, 94*, pp.307-314.
634 Line, L., Alhede, M., Kolpen, M., Kühl, M., Ciofu, O., Bjarnsholt, T., Moser, C., Toyofuku,
635 M., Nomura, N., Høiby, N. and Jensen, P.Ø. (2014). Physiological levels of nitrate support
636 anoxic growth by denitrification of Pseudomonas aeruginosa at growth rates reported in cystic
637 fibrosis lungs and sputum. *Frontiers in microbiology*, *5*, 554.

638 Little, B.J., Blackwood, D.J., Hinks, J., Lauro, F.M., Marsili, E., Okamoto, A., Rice, S.A.,
639 Wade, S.A. and Flemming, H.C. (2020). Microbially influenced corrosion—any
640 progress?. *Corrosion Science*, *170*, 108641.

641 Ma, R., Wang, G., Tian, Y., Wang, K., Zhang, J., Fang, J. (2015). Non-thermal plasma-
642 activated water inactivation of food-borne pathogen on fresh produce. *Journal of hazardous*
643 *materials*, *300*, 643-651.

644 Mai-Prochnow, A., Zhou, R., Zhang, T., Ostrikov, K. K., Mugunthan, S., Rice, S. A., Cullen,
645 P. J. (2021a). Interactions of plasma-activated water with biofilms: inactivation, dispersal
646 effects and mechanisms of action. *NPJ biofilms and microbiomes*, *7*(1), 1-12.

647 Mai-Prochnow, A., Alam, D., Zhou, R., Zhang, T., Ostrikov, K., Cullen, P. J. (2021b).
648 Microbial decontamination of chicken using atmospheric plasma bubbles. *Plasma Processes*
649 *and Polymers*, 18(1), 2000052.

650 Mai-Prochnow, A., Evans, F., Dalisay-Saludes, D., Stelzer, S., Egan, S., James, S., Webb, J.S.
651 and Kjelleberg, S. (2004). Biofilm development and cell death in the marine bacterium
652 *Pseudoalteromonas tunicata*. *Applied and environmental microbiology*, *70*(6), pp.3232-3238.

653 Maxwell, S. (2006). Predicting Microbiologically Influenced Corrosion (MIC) in seawater
654 systems. *2006 SPE International Oil Field Corrosion Symposium*, Aberdeen, UK: Society of
655 Petroleum Engineers.

656 Meireles, A., Giaouris, E., Simões, M. (2016). Alternative disinfection methods to chlorine for
657 use in the fresh-cut industry. *Food Research International*, *82*, 71-85.

658 Morales, J., Esparza, P., Gonzalez, S., Salvarezza, R. Arevalo, M. P. (1993). The role of
659 *Pseudomonas aeruginosa* on the localised corrosion of 304 stainless steel. *Corrosion science*,
660 *34*(9), 1531-1540.

661 Myszka, K., Czaczyk, K. (2011). Bacterial biofilms on food contact surfaces-a review. *Polish*
662 *Journal of Food and Nutrition Sciences*, *61*(3).

Naidis, G.V. (2010). Modelling of streamer propagation in atmospheric-pressure helium plasma jets. *Journal of Physics D: Applied Physics, 43*(40), p.402001.

Naïtali, M., Kamgang-Youbi, G., Herry, J. M., Bellon-Fontaine, M. N., & Brisset, J. L. (2010). Combined effects of long-living chemical species during microbial inactivation using atmospheric plasma-treated water. *Applied and environmental microbiology*, *76*(22), 7662-7664.

Oehmigen, K., Winter, J., Hähnel, M., Wilke, C., Brandenburg, R., Weltmann, K. D., & von Woedtke, T. (2011). Estimation of possible mechanisms of *Escherichia coli* inactivation by plasma treated sodium chloride solution. *Plasma Processes and Polymers*, *8*(10), 904-913.

Ogden, T. L. (2010). Handling results below the level of detection. *The Annals of occupational hygiene*, *54*(3), 255-256.

Pan, J., Li, Y.L., Liu, C.M., Tian, Y., Yu, S., Wang, K.L., Zhang, J. and Fang, J. (2017). Investigation of cold atmospheric plasma-activated water for the dental unit waterline system contamination and safety evaluation in vitro. *Plasma Chemistry and Plasma Processing*, *37*(4), pp.1091-1103.

Papagianeli, S. D., Aspridou, Z., Didos, S., Chochlakis, D., Psaroulaki, A., & Koutsoumanis, K. (2021). Dynamic modelling of Legionella pneumophila thermal inactivation in water. *Water Research*, *190*, 116743.

Park, J. Y., Park, S., Choe, W., Yong, H. I., Jo, C., Kim, K. (2017). Plasma-functionalized solution: A potent antimicrobial agent for biomedical applications from antibacterial therapeutics to biomaterial surface engineering. *ACS applied materials and interfaces*, 9(50), 43470-43477.

Patange, A. D., Simpson, J. C., Curtin, J. F., Burgess, C. M., Cullen, P. J., & Tiwari, B. K. (2021). Inactivation efficacy of atmospheric air plasma and airborne acoustic ultrasound against bacterial biofilms. *Scientific Reports*, *11*(1), 1-14.

688 Pasquali, F., Stratakos, A.C., Koidis, A., Berardinelli, A., Cevoli, C., Ragni, L., Mancusi, R.,
689 Manfreda, G. and Trevisani, M. (2016). Atmospheric cold plasma process for vegetable leaf
690 decontamination: A feasibility study on radicchio (red chicory, Cichorium intybus L.). *Food*
691 *control*, *60*, pp.552-559.
692 Phan, H. C., Blackall, L. L., & Wade, S. A. (2021). Effect of Multispecies Microbial Consortia
693 on Microbially Influenced Corrosion of Carbon Steel. *Corrosion and Materials*
694 *Degradation*, *2*(2), 133-149.
695 Pinto, R. M., Soares, F. A., Reis, S., Nunes, C., Van Dijck, P. (2020). Innovative strategies
696 toward the disassembly of the EPS matrix in bacterial biofilms. *Frontiers in Microbiology*, 11.
697 Qian, J., Ma, L., Yan, W., Zhuang, H., Huang, M., Zhang, J. and Wang, J. (2021). Inactivation
698 kinetics and cell envelope damages of foodborne pathogens Listeria monocytogenes and
699 Salmonella Enteritidis treated with cold plasma. *Food Microbiology*, p.103891.
700 Robert, E., Darny, T., Dozias, S., Iseni, S. and Pouvesle, J.M. (2015). New insights on the
701 propagation of pulsed atmospheric plasma streams: From single jet to multi jet arrays. *Physics*
702 *of plasmas*, *22*(12), p.122007.
703 Sadiq, M. B., Tarning, J., Aye Cho, T. Z., Anal, A. K. (2017). Antibacterial activities and
704 possible modes of action of Acacia nilotica (L.) Del. against multidrug-resistant Escherichia
705 coli and Salmonella. *Molecules*, *22*(1), 47.
706 Shen, J., Tian, Y., Li, Y., Ma, R., Zhang, Q., Zhang, J., and Fang, J. (2016). Bactericidal effects
707 against S. aureus and physicochemical properties of plasma activated water stored at different
708 temperatures. *Scientific reports*, *6*(1), 1-10.
709 Silvestri, E.E., Yund, C., Taft, S., Bowling, C.Y., Chappie, D., Garrahan, K., Brady-Roberts,
710 E., Stone, H., and Nichols, T.L. (2017). Considerations for estimating microbial environmental
711 data concentrations collected from a field setting. *Journal of Exposure Science and*
712 *Environmental epidemiology*, *27*(2), 141-151.

713 Skovhus, T. L., Taylor, C., Eckert, R. B. (2019). Modeling of Microbiologically influenced
714 corrosion – Limitations and perspectives. *CRC press*.
715 Smet, C., Govaert, M., Kyrylenko, A., Easdani, M., Walsh, J. L., Van Impe, J. F. (2019).
716 Inactivation of single strains of Listeria monocytogenes and Salmonella typhimurium
717 planktonic cells biofilms with plasma activated liquids. *Frontiers in microbiology*, *10*, 1539.
718 Smith, K., Rajendran, R., Kerr, S., Lappin, D. F., Mackay, W. G., Williams, C., & Ramage, G.
719 (2015). Aspergillus fumigatus enhances elastase production in Pseudomonas aeruginosa co-
720 cultures. *Medical mycology*, *53*(7), 645-655.
721 Stratakos, A.C., Sima, F., Ward, P., Linton, M., Kelly, C., Pinkerton, L., Stef, L., Pet, I. and
722 Corcionivoschi, N. (2018). The in vitro effect of carvacrol, a food additive, on the pathogenicity
723 of O157 and non-O157 Shiga-toxin producing Escherichia coli. *Food Control*, *84*, pp.290-296.
724 Su P., Fuller D.B. (2014). Corrosion and corrosion mitigation in fire protection systems,
725 *Research Technical Report FM Global*.
726 Surowsky, B., Bußler, S., & Schlüter, O. K. (2016). Cold plasma interactions with food
727 constituents in liquid and solid food matrices. In *Cold plasma in food and agriculture* (pp. 179-
728 203). Academic Press.
729 Tan, J., Karwe, M. V. (2021). Inactivation and removal of Enterobacter aerogenes biofilm in a
730 model piping system using plasma-activated water (PAW). *Innovative Food Science &*
731 *Emerging Technologies*, *69*, 102664.
732 Thirumdas, R., Kothakota, A., Annapure, U., Siliveru, K., Blundell, R., Gatt, R., &
733 Valdramidis, V. P. (2018). Plasma activated water (PAW): Chemistry, physico-chemical
734 properties, applications in food and agriculture. *Trends in food science & technology*, *77*, 21-
735 31.
736 Thorman, R.E., Nicholson, F.A., Topp, C.F., Bell, M.J., Cardenas, L.M., Chadwick, D.R.,
737 Cloy, J.M., Misselbrook, T.H., Rees, R.M., Watson, C.J. and Williams, J.R. (2020). Towards

738 country-specific nitrous oxide emission factors for manures applied to arable and grassland
739 soils in the UK. *Frontiers in Sustainable Food Systems*, *4*, p.62.
740 Tian, Y., Ma, R., Zhang, Q., Feng, H., Liang, Y., Zhang, J. and Fang, J., 2015. Assessment of
741 the physicochemical properties and biological effects of water activated by non-thermal plasma
742 above and beneath the water surface. *Plasma processes and polymers*, *12*(5), pp.439-449.
743 Wang, W., Wang, J., Li, X., Xu, H., Wu, J. (2004). Influence of biofilms growth on corrosion
744 potential of metals immersed in seawater. *Materials Corrosion–Werkstoffe Korrosion*, 55, 30-
745 35.
746 Vijayarangan, V., Delalande, A., Dozias, S., Pouvesle, J.M., Robert, E. and Pichon, C. (2020).
747 New insights on molecular internalization and drug delivery following plasma jet exposures.
748 *International Journal of Pharmaceutics*, *589*, p.119874.
749 Xiang, Q., Kang, C., Niu, L., Zhao, D., Li, K., & Bai, Y. (2018). Antibacterial activity and a
750 membrane damage mechanism of plasma-activated water against *Pseudomonas deceptionensis*
751 CM2. *LWT*, *96*, 395-401.
752 Xu, D., Xia, J., Zhou, E., Zhang, D., Li, H., Yang, C., Li, Q., Lin, H., Li, X. and Yang, K.
753 (2017). Accelerated corrosion of 2205 duplex stainless steel caused by marine aerobic
754 *Pseudomonas aeruginosa* biofilm. *Bioelectrochemistry*, *113*, pp.1-8.
755 Xu, D., Li, Y., & Gu, T. (2016). Mechanistic modeling of biocorrosion caused by biofilms of
756 sulfate reducing bacteria and acid producing bacteria. *Bioelectrochemistry*, *110*, 52-58.
757 Yuan, S. J., Pehkonen, S. O., Ting, Y. P., Kang, E. T., Neoh, K. G. (2008). Corrosion behavior
758 of type 304 stainless steel in a simulated seawater-based medium in the presence and absence
759 of aerobic Pseudomonas NCIMB 2021 bacteria. *Industrial and engineering chemistry*
760 *research*, *47*(9), 3008-3020.

761 Yuan, S. J., Choong, A. M., Pehkonen, S. O. (2007). The influence of the marine aerobic
762 Pseudomonas strain on the corrosion of 70/30 Cu–Ni alloy. *Corrosion science*, *49*(12), 4352-
763 4385.
764 Zhao, Y.M., Ojha, S., Burgess, C.M., Sun, D.W. and Tiwari, B.K. (2020). Inactivation efficacy
765 and mechanisms of plasma activated water on bacteria in planktonic state. *Journal of applied*
766 *microbiology*, *129*(5), pp.1248-1260.
767 Zhang, Q., Zhuang, J., von Woedtke, T., Kolb, J.F., Zhang, J., Fang, J. and Weltmann, K.D.
768 (2014). Synergistic antibacterial effects of treatments with low temperature plasma jet and
769 pulsed electric fields. *Applied Physics Letters*, *105*(10), p.104103.
770 Zhou, R., Zhou, R., Wang, P., Xian, Y., Mai-Prochnow, A., Lu, X., Cullen, P.J., Ostrikov, K.K.
771 and Bazaka, K. (2020). Plasma-activated water: generation, origin of reactive species and
772 biological applications. *Journal of Physics D: Applied Physics*, *53*(30), p.303001.
773 Zhou, R., Zhou, R., Prasad, K., Fang, Z., Speight, R., Bazaka, K., Ostrikov, K. K. (2018). Cold
774 atmospheric plasma activated water as a prospective disinfectant: the crucial role of
775 peroxynitrite. *Green Chemistry*, *20*(23), 5276-5284.

FIGURE LEGENDS

FIGURE 1. Schematic representation of the PBR used to generate the PAW consisting of an acrylic tube submerged into water, high-voltage power supply to generate atmospheric plasma under atmospheric conditions and supply of compressed air at a flow rate of 1 L/min.

FIGURE 2. Reduction of *P. aeruginosa* planktonic cells after 5, 10, and 15 min of exposure to PAW at PBR discharge frequencies of 500, 1000, and 1500 Hz. Each bar represents the mean value of three replicates, each of which was analyzed twice. The error bars represent the Standard Deviation for Mean (n = 6). The values with uppercase letters followed by the same lowercase letters did not differ significantly between the exposure times ($P > 0.05$). The values with uppercase letters followed by different lowercase letters differed significantly between exposure times ($P < 0.05$). Asterisk (*) indicates the values which were below the detection limit (1.00 Log CFU ml^{-1})

FIGURE 3. Reduction of *P. aeruginosa* biofilms of different maturity (24, 48, and 72 h) after 5, 10, 15, and 20 min of exposure during PAW treatment at 1500 Hz. Each bar represents the mean value of three replicates, each of which was analyzed twice. The error bars represent the Standard Deviation for Mean (n = 6). The values with uppercase letters followed by the same lowercase letters did not differ significantly between the exposure times ($P > 0.05$). The values with uppercase letters followed by different lowercase letters differed significantly between exposure times ($P < 0.05$). Asterisk (*) indicates the values which were below the detection limit (2.00 Log CFU $cm^{2\ -1}$)

FIGURE 4. Release of proteins from *P. aeruginosa* Control (untreated cells) and from cells treated with PAW at PBR discharge frequencies of 500, 1000, and 1500 Hz. The error bars represent the Standard Deviation for Mean (n = 3). The treatments with different lowercase letters differ significantly ($P < 0.05$)

FIGURE 5. Intracellular ATP production by *P. aeruginosa* untreated (Control) and by the cells treated with PAW at different PBR discharge frequencies. The error bars represent the Standard Deviation for Mean (n = 3). The treatments with different lowercase letters differ significantly ($P < 0.05$)

FIGURE 6. Inactivation curves of *P. aeruginosa* biofilms of different maturity under the treatment with 1500 Hz frequency. Censored data were handled using a substitution method, using half the detection limit. Each point represents the mean value of six replicates

FIGURE 7. Inactivation curves of *P. aeruginosa* planktonic cells after 5, 10, and 15 min of exposure during PAW treatment at PBR discharge frequencies of 500, 1000, and 1500 Hz. Censored data were handled using a substitution method, using half the detection limit. Each point represents the mean value of six replicates

TABLE 1. Physicochemical parameters and reactive molecular species in PAW after 15 min exposure at 1500 Hz

Treatments	pH	EC ($mS\ cm^{-1}$)	H_2O_2 ($mg\ ml^{-1}$)	NO_2^- ($mg\ ml^{-1}$)	NO_3^- ($mg\ ml^{-1}$)
Tap water*	7.56 ± 0.02^A	230.667 ± 2.73^A	-	-	-
PAW	5.94 ± 0.04^B	325.333 ± 11.64^B	0.03±0.002	0.04± 0.001	0.04±0.001

*Tap water prior to the use of PBR to generate PAW.

The results are presented as mean ± standard deviation (SD). The mean values were calculated for three replicates, each of which was analyzed twice (n=6).

Values in the same column with different uppercase letters differ significantly ($P < 0.05$).

TABLE 2. Model parameters and associated errors for biofilm cells of different maturity (24, 48, and 72 h) after 5, 10 and 15 of exposure to PAW treatment at 1500 Hz

Biofilm maturity (h)	Parameters							
	D_T	SE	$logN_o$	SE	Mean Sum of R^2	R^2 Root Mean Sum	R^2	R^2 adjusted
24	3.11	0.13	5.51	0.53	0.3965	0.6296	0.9417	0.9125
48	4.34	0.09	5.67	0.46	0.3507	0.5922	0.9253	0.9005
72	4.19	0.07	6.21	0.36	0.2102	0.4585	0.9548	0.9445

TABLE 3. Model parameters and associated errors of *P. aeruginosa* planktonic cells after 5, 10, and 15 min of exposure during PAW treatment at PBR discharge frequencies of 500, 1000, and 1500 Hz

PBR discharge frequencies (Hz)	Parameters							
	D_T	SE	$logN_o$	SE	Mean Sum of R^2	R^2 Root Mean Sum	R^2	R^2 adjusted
500	8.53	0.02	5.03	0.10	0.0147	0.1213	0.9833	0.9749
1000	3.44	0.04	4.89	0.16	0.0374	0.1933	0.9930	0.9895
1500	2.24	0.07	4.90	0.20	0.0479	0.2188	0.9953	0.9906

834 **FIG 1**

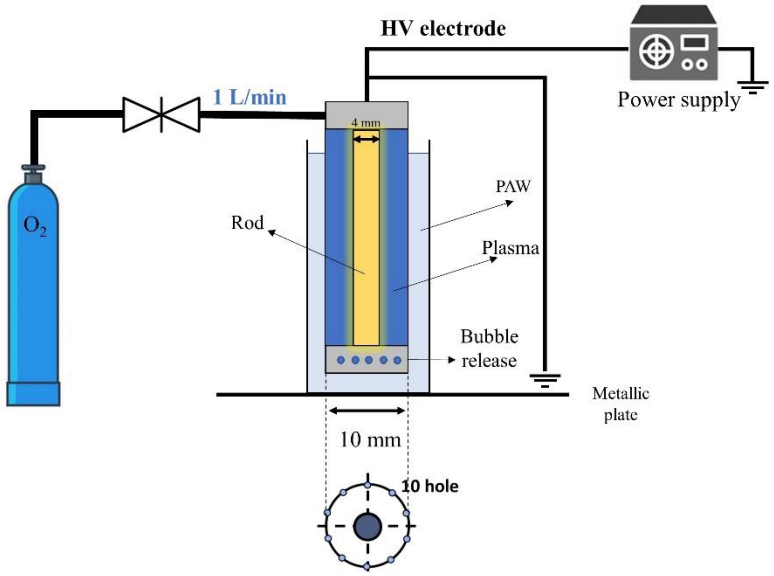

835

836 **FIG 2**

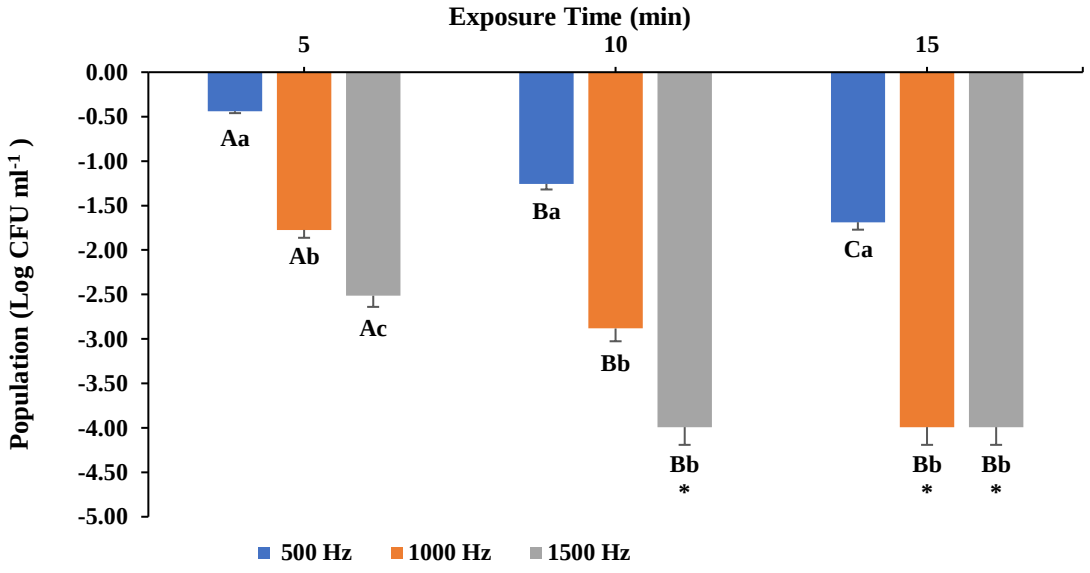

837

838

839

840

841

842

843 **FIG 3**

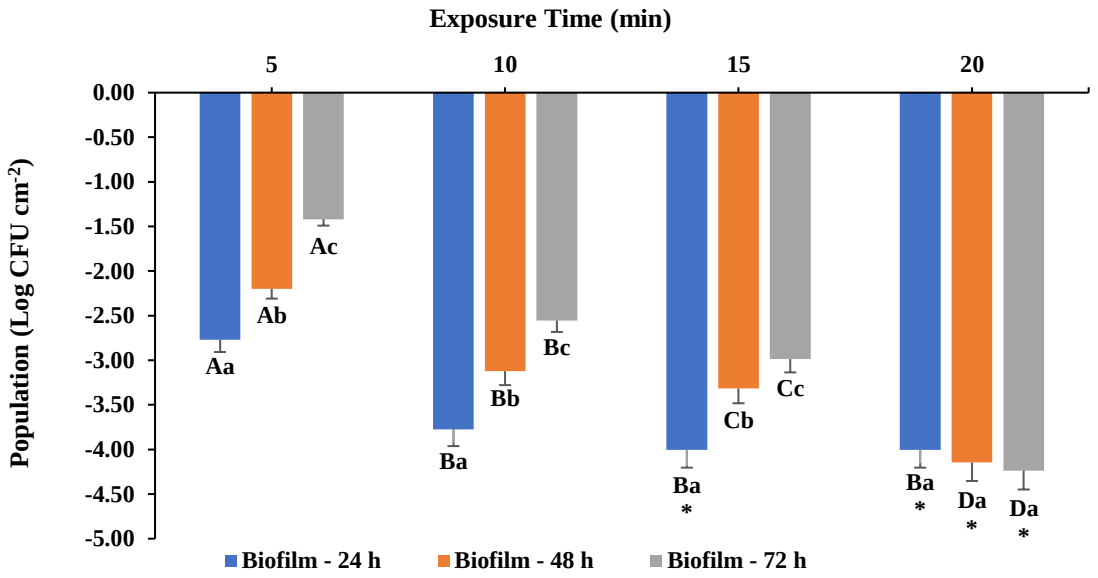

844

845 **FIG 4**

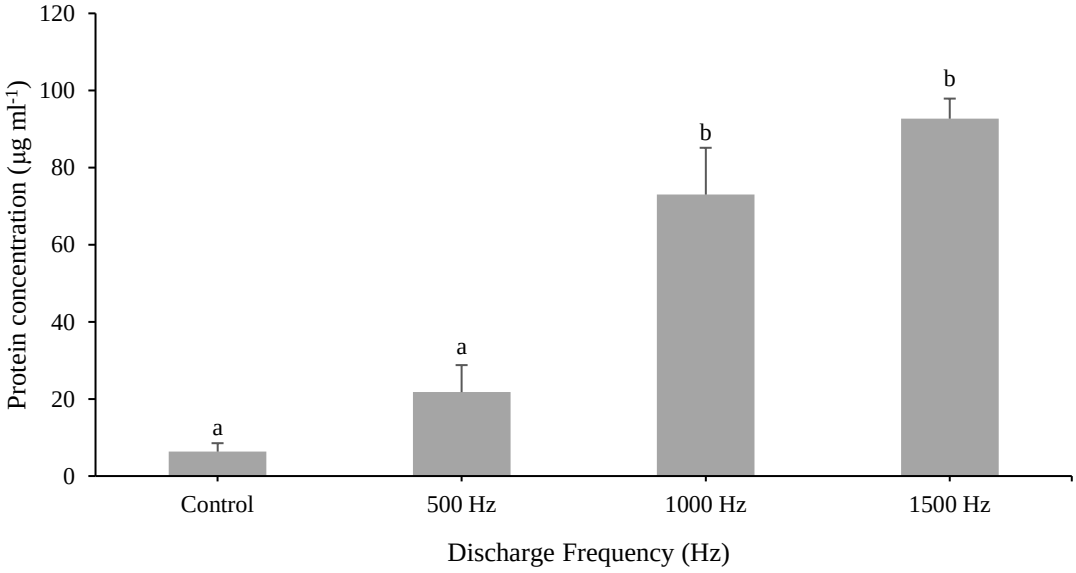

846

847

848

849

850

851

852

FIG 5

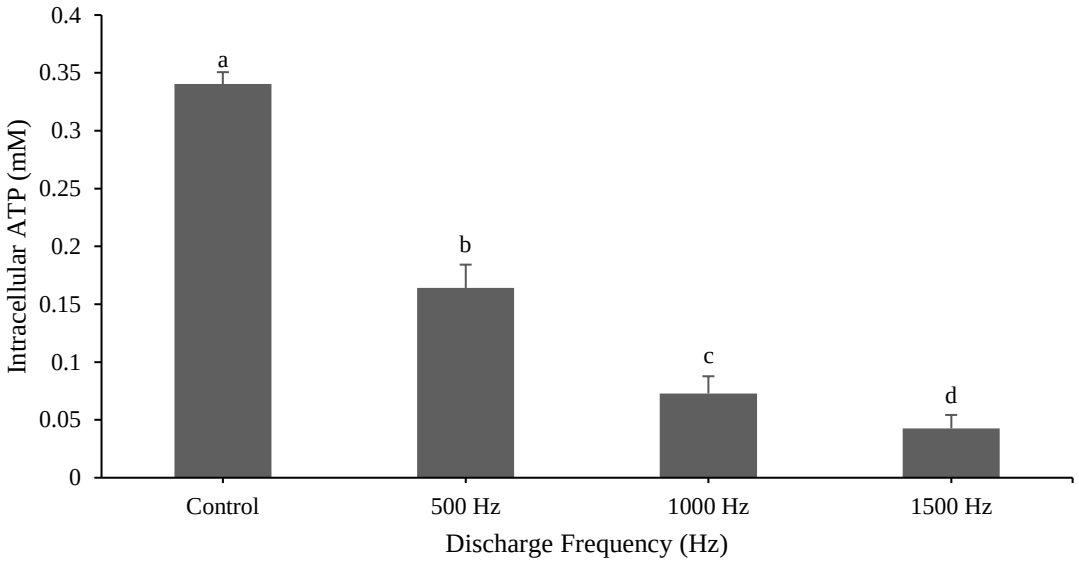
Intracellular ATP (mM)
0.4
0.35
0.3
0.25
0.2
0.15
0.1
0.05
0
a
b
c
d
Control
500 Hz
1000 Hz
1500 Hz
Discharge Frequency (Hz)

FIG 6

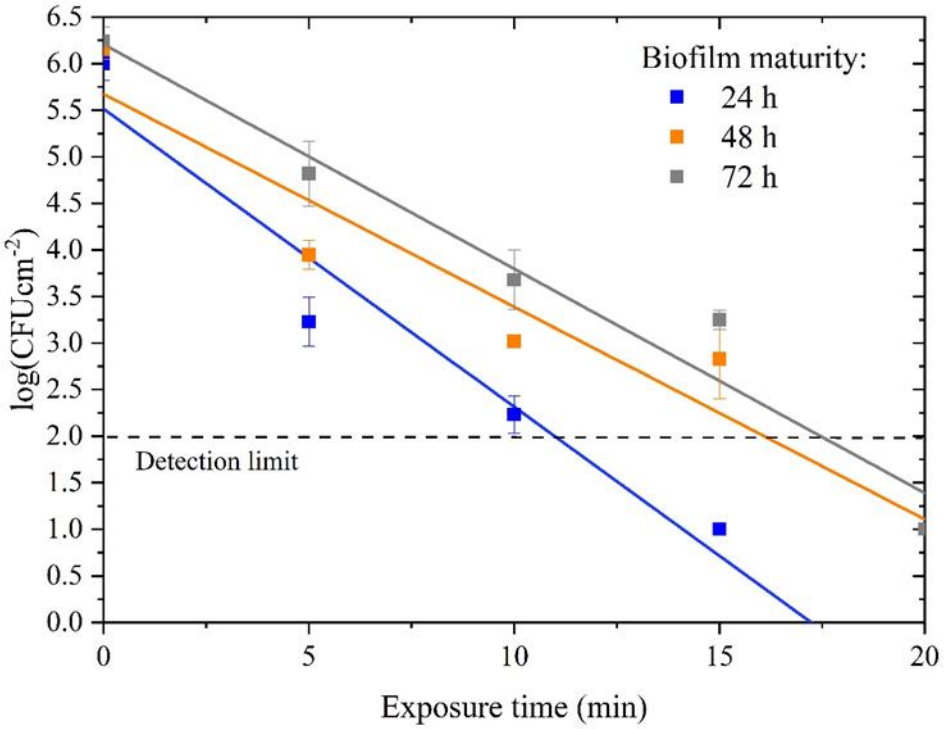
log(CFUcm-2)
6.5
6.0
5.5
5.0
4.5
4.0
3.5
3.0
2.5
2.0
1.5
1.0
0.5
0.0
Biofilm maturity:
24 h
48 h
72 h
Detection limit
0
5
10
15
20
Exposure time (min)

860 **FIG 7**

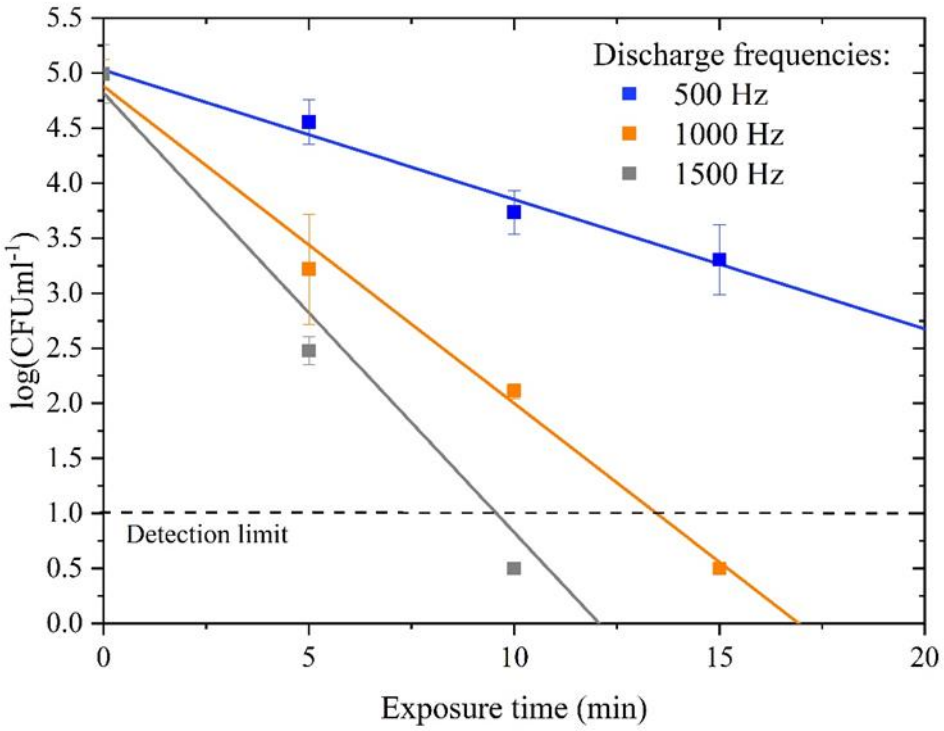

861

862

863

864